

# ICSV14

Cairns • Australia  
9-12 July, 2007



## COMPARISON OF EXPERIMENT, FINITE ELEMENT AND WAVE BASED MODELS FOR MASS INCLUSIONS IN PORO-ELASTIC LAYERS

M. R. F. Kidner<sup>\*1</sup>, Kamal Idrisi<sup>2</sup>, J. P. Carneal<sup>2</sup> and M. E. Johnson<sup>2</sup>

<sup>1</sup>Acoustics, Vibration & Control Group, Dept of Mechanical Engineering The University of  
Adelaide Australia 5005

<sup>2</sup>Vibration and Acoustics Laboratory Dept. of Mechanical Engineering, Virginia Polytechnic  
Institute and State University Blacksburg VA 24061 USA

[mike.kidner@mecheng.adelaide.edu.au](mailto:mike.kidner@mecheng.adelaide.edu.au) (e-mail address of lead author)

### Abstract

The addition of small mass inclusions into the poro-elastic layer was found to create an increase in insertion loss (IL) over a broadband frequency range, usually below 1000 Hz. In this paper, results of two models: a simplified closed form approximation to the frame dynamics and a fully couple finite element analysis, are compared to experimental results. The motivation is the large computational effort that is required by the fully coupled 3-D finite element model of the poro-elastic material makes optimization prohibitive in terms of time/computational power. Proof of equivalency of the analytical approximation, the FEA model and experimental data allows the former to be used in the optimization of inclusion design. Results from the fully coupled 3-D model, an approximation to the Biot model, and an experimental investigation are compared and discussed.

### 1. Introduction

This paper concerns a relatively new approach to improving transmission loss, the Heterogeneous Blanket (HG-blanket). Previous experimental work, [1] showed that a wide bandwidth enhancement in the transmission loss could be achieved by adding many small mass inclusions to a poro-elastic layer attached to a panel. Each of the mass inclusions behaves like a vibration absorber so that there is an overall increase in the panel impedance over the bandwidth of the inclusions resonances. An equivalent single-degree of freedom stiffness was derived [2] from the Biot-Allard equations, [3, 4]. The equivalent stiffness was validated by experimental measurements. In this paper we extend the analysis to include a finite element model of the poro-elastic layer.

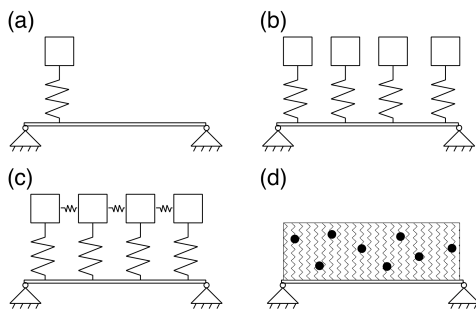


Figure 1. Development of the mass-inclusion concept

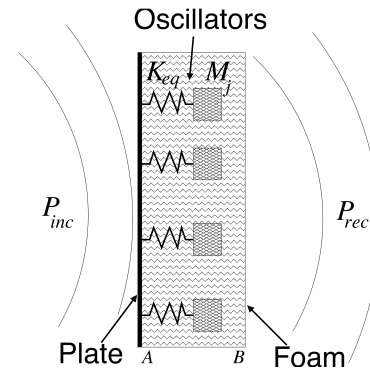


Figure 2. Schematic of the model of a plate with foam layer and inclusions modelled as oscillators.

In 1977 Craggs proposed a finite element scheme for porous liners, however he neglected the elasticity of the frame material. This is a valid assumption for many sound absorption applications but completely invalid for modelling the HG-blanket. Inclusions of fluid have been considered by researchers in the geo-mechanics field such as Kostek, [5], however it was not until 1994 that an elastic frame was considered. [6]. This led to a flurry of activity in finite element modelling of poro-elastic materials. The key players in the field being: Atalla [7, 8, 9], Panneton [10],[11] and Kang [6, 12, 13].

Panneton and Atalla,[10] proposed an efficient method for solving the  $\underline{u} - \underline{U}$  finite element formulation by linearising the frequency dependency of the stiffness and damping matrices. This is the approach followed in the model developed here.

The HG blanket evolved from the application of vibration absorbers to transmission loss through fuselage and fairings, where a relatively low weight, high TL, and practical solution is sort. Transmission through aircraft and rocket has been a subject for the application of active control, adaptive passive control, ASAC *etc.* for many years [14, 15, 16]. The application of vibration absorbers to the problem has received much attention and is reviewed by Kidner and Wright [17] and by Sun [18].

Figure 1 illustrates the evolution of a traditional point absorber to a random collection of masses embedded within a poro-elastic layer. The use of a single point absorber, Figure 1-a was extended to multiple absorbers acting over a distributed space, Figure 1-b, an example of this is work by [19]. Coupling between the absorber masses was then considered, as shown in Figure 1-c. This coupling has been discussed in work on the effective impedance of collections of oscillators, by [20] and [21]. The extension to continuous elastic layer with embedded masses, Figure 1-d comes from work by [22] and [15] on distributed vibration absorbers.

Figure 2 is a schematic of the combination of plate, foam layer and mass inclusions. It shows the mass inclusions modelled as separate mass-spring oscillators. The stiffness and damping of these oscillators is derived from the Biot equations in section 4.. It is assumed that the mass inclusions do not couple to the acoustic field. The effect of the oscillators of the poro-elastic layer is considered as a separate problem. The finite element approach solves the fully coupled problem, and as such can be used to predict the effects of more complex geometries and features such as macroscopic voids in the porous layer.

## 1.1 Paper Structure

Following this introduction the physics of poro-elastic materials are reviewed and the finite element method for analysis of porous mediums is introduced. The  $\underline{u} - \underline{U}$  approach used is outlined and the MatLab model explained. In section 4, the wave approach to modeling is reviewed and an equivalent stiffness and damping value obtained for a small element of porous material. The equivalency to the FEA stiffness matrix is shown. The penultimate section is a discussion of the results and the paper closes with the conclusions.

## 2. Review of poro-elastic material physics

A poro-elastic medium has two phases, a fluid and an elastic frame. Biot [23] derived the stress-strain relationships as

$$\sigma_i = 2Ne_i + Ae + Q\epsilon, \quad (1)$$

where  $i = x, y, z$ . The total volumetric strain of the frame,  $e$  is given by the divergence of the displacement vector  $\underline{u}$ . The fluid volumetric strain  $\epsilon$  is given by the divergence of the fluid displacement field  $\underline{U}$ .  $N$  denotes the shear modulus and  $A$  is the first Lamé coefficient, defined as  $A = \nu E / [(1 + \nu)(1 - 2\nu)]$ , where  $\nu$  denotes Poission's ratio and  $E$  is the Young's modulus of the frame material.  $Q$  is defined below.

Biot then defines the fluid stress,  $s$ , (or negative pressure) as:

$$s = R\epsilon + Qe. \quad (2)$$

Here  $R$  is a measure of the pressure required to force a portion of the fluid into the fluid-frame aggregate while maintaining a constant aggregate volume, [23]. The constant  $Q$  relates the volume changes of the fluid to that of the frame and is defined by  $Q/R = -\epsilon/e$ .

To derive dynamic equations the inertial coupling between the fluid and the frame must be defined. Biot derives the following expressions to accomodate this coupling:

$$\begin{aligned} \rho_{11}^* &= \rho_{11} + \frac{b}{j\omega} & \rho_{11} &= \rho_s + \rho_a \\ \rho_{12}^* &= \rho_{12} - \frac{b}{j\omega} & \rho_{12} &= -\rho_a \\ \rho_{22}^* &= \rho_{22} + \frac{b}{j\omega} & \rho_{22} &= \rho_f + \rho_a \end{aligned} \quad (3)$$

Each of the effective densities  $\rho_{11}$ ,  $\rho_{12}$  and  $\rho_{22}$  contribute to the inertial coupling as follows:

- The mass of the fluid that couples to the motion of the frame,  $-\rho_a$ ;
- The effective moving mass of the frame, which is its actual mass plus the mass of the fluid that moves with it,  $(\rho_{11} + \rho_a)$ ;
- The effective moving mass of the fluid,  $(\rho_{22} + \rho_a)$ .

The starred quantities include the viscous damping effects modeled by a complex term  $b/j\omega$ .  $\rho_a$ , the inertial coupling, is a function of the structural factor  $\beta$ , and the fluid density  $\rho_f$ .

$$\rho_a = (1 - \beta)\rho_f$$

The structural density is  $\rho_s$ .

The viscous losses represented by  $b$  are a function of the assumed pore geometry. There are several models for this value. In this work the following is used [24]:

$$b(\omega) = j\omega\rho_f\beta \frac{2J_1(\lambda_c\sqrt{-j})}{\lambda_c\sqrt{-j} J_0(\lambda_c\sqrt{-j})} \left(1 - \frac{2J_1(\lambda_c\sqrt{-j})}{\lambda_c\sqrt{-j} J_0(\lambda_c\sqrt{-j})}\right)^{-1} \quad (4)$$

$$\lambda_c = \sqrt{\frac{8\omega\rho_f\beta}{\phi\chi}},$$

where  $\chi$  is the flow resistivity,  $\omega$  is the frequency in radians.

### 3. The finite element for poro-elastic materials

Panneton and Atalla [25] use a Lagrangian approach to develop the finite element equations for a poroelastic element. It is first necessary to define the stress, strain, and displacement vectors:  $\boldsymbol{\sigma}_s = [\sigma_x \ \sigma_y \ \sigma_z \ \tau_{xy} \ \tau_{yz} \ \tau_{zx}]^T$  The previous stress vector is for the solid portion of the poroelastic element which supports both normal and shear stresses. The following stress vector is for the fluid portion of the element and can only have a normal stress which is equal to the porosity multiplied by the applied force.  $\boldsymbol{\sigma}_f = [-\phi p \ -\phi p \ -\phi p \ 0 \ 0 \ 0]^T$  Where  $\phi$  is the porosity of the material and  $p$  is the pressure on the surface. There are six degrees of freedom for each node on a poroelastic element and they represent the three cartesian co-ordinates for the fluid and three cartesian co-ordinates for the frame. We will find that coupling equations are necessary to allow these elements to be used with traditional solid and fluid finite elements which each have three degrees of freedom.  $\mathbf{u}_s = [u_{sx} \ u_{sy} \ u_{sz}]^T$   $\mathbf{u}_f = [u_{fx} \ u_{fy} \ u_{fz}]^T$  The strains  $\boldsymbol{\epsilon}$  are written in terms of the derivatives of the displacements.  $\boldsymbol{\epsilon}_s = [\mathbf{L}][\mathbf{u}_s]$  and  $\boldsymbol{\epsilon}_f = [\mathbf{L}][\mathbf{u}_f]$  Where  $[\mathbf{L}]$  is the derivative operator.

Expressions relating the fluid and frame stresses to the strains are given in Equations (5) and (6). These follow the form of Equations (1) and (2) in that they involve both frame and fluid strains.

$$\boldsymbol{\sigma}_s = \mathbf{D}_s\boldsymbol{\epsilon}_s + \mathbf{D}_{sf}\boldsymbol{\epsilon}_f \quad (5)$$

$$\boldsymbol{\sigma}_f = \mathbf{D}_f\boldsymbol{\epsilon}_f + \mathbf{D}_{sf}\boldsymbol{\epsilon}_s \quad (6)$$

In the above equations  $\mathbf{D}_s$  is determined from the coefficients  $A$  and  $N$ .  $\mathbf{D}_{sf}$  is dependent on the elastic coupling between the fluid and the frame,  $Q$ .  $\mathbf{D}_f$  is depends on  $R$ .

An energy balance in the form of a modified Lagrangian is used to obtain the equation of motion for the poroelastic material. The standard Lagrangian equation had to be modified to allow for a dissipation term. Expressions for the kinetic energy, strain energy, dissipation energy, and external work are given in Equations (7-10).

Kinetic Energy:

$$dT = \frac{1}{2} (\rho_{11}\dot{\mathbf{u}}_s^T \dot{\mathbf{u}}_s + 2\rho_{12}\dot{\mathbf{u}}_s^T \dot{\mathbf{u}}_f + \rho_{22}\dot{\mathbf{u}}_f^T \dot{\mathbf{u}}_f) \quad (7)$$

Strain Energy:

$$dU = \frac{1}{2} \left[ [\mathbf{L}\mathbf{u}_s]^T \mathbf{D}_s [\mathbf{L}\mathbf{u}_s] + 2[\mathbf{L}\mathbf{u}_s]^T \mathbf{D}_{sf} [\mathbf{L}\mathbf{u}_f] + [\mathbf{L}\mathbf{u}_f]^T \mathbf{D}_f [\mathbf{L}\mathbf{u}_f] \right] \quad (8)$$

Dissipation Energy:

$$dD = \frac{b(\omega)}{2} (\dot{\mathbf{u}}_s - \dot{\mathbf{u}}_f)^T (\dot{\mathbf{u}}_s - \dot{\mathbf{u}}_f) \quad (9)$$

Work Energy:

$$dW = \mathbf{u}_s^T (\mathbf{f} - h\mathbf{f}_n) + h\mathbf{u}_f^T \mathbf{f}_n, \quad (10)$$

where  $\mathbf{f}$  and  $\mathbf{f}_n$  are the force and the corresponding normal force respectively that act on the external surface of the poroelastic material. The modified Lagrangian equation, modified to accommodate dissipation is shown below. Where the modified Lagrangian is given by:

$$\frac{dT - dU}{d\dot{\mathbf{u}}} - \frac{dT - dU}{d\mathbf{u}} + \frac{dD}{d\dot{\mathbf{u}}} = \frac{dW}{d\mathbf{u}} \quad (11)$$

Where  $\mathbf{u} = [\mathbf{u}_s \mathbf{u}_f]^T$ . The Lagrangian equation above can be integrated and rearranged to reveal the equation of motion for a poroelastic element:

$$\left( -\omega^2 \begin{bmatrix} M_{ss} & M_{sf} \\ M_{sf} & M_{ff} \end{bmatrix} + j\omega \begin{bmatrix} C_{ss}(\omega) & C_{sf}(\omega) \\ C_{sf}(\omega) & C_{ff}(\omega) \end{bmatrix} + \begin{bmatrix} K_{ss} & K_{sf}(\omega) \\ K_{sf}(\omega) & K_{ff}(\omega) \end{bmatrix} \right) \begin{bmatrix} \mathbf{u}_s \\ \mathbf{u}_f \end{bmatrix} = \begin{bmatrix} \mathbf{F}_s \\ \mathbf{F}_f \end{bmatrix} \quad (12)$$

In Equation (12), the mass matrix ( $\mathbf{M}$ ) is a function of the densities ( $\rho_{11}, \rho_{12}, \rho_{22}$ ) of the frame and fluid, the damping matrix ( $\mathbf{C}$ ) is a function of the damping function ( $b(\omega)$ ), and the stiffness matrix ( $\mathbf{K}$ ) is in terms of  $\mathbf{D}_s$ ,  $\mathbf{D}_f$ , and  $\mathbf{D}_{sf}$ .

To simplify the computation Panneton introduces a low frequency approximations for the damping and stiffness. This depends on *characteristic dimensions* that relate the pore size and viscosity.

The finite element model was implemented in C++ using the LibMesh finite element library [26]. The low frequency simplifications for the damping and stiffness terms as specified by Panneton [10] were implemented. In the results presented a 1D model was created containing 10 elements. The element size was approximately 10mm. The mass inclusion was implemented as an increase in density at the element of interest. A typical result for the input mechanical impedance to the foam block is shown in Figure 3, it can be seen that the resonances vary from 95 to 200Hz.

#### 4. Equivalent stiffness of a foam layer

Figure 5 shows the stresses and strains that can exist in a poro-elastic material. The motion of the structure and the fluid is coupled. The stress in the  $x$ -direction in the frame,  $\sigma_x$ , is due to both solid and acoustic strains as shown in Equation 1. The fluid stress is defined in Equation 2. To obtain an equivalent stiffness of a column of porous material both the structure and fluid is considered. The force balance equation for the foam block shown in Figure 5 is

$$S(\sigma_x + \sigma_f) = K_{eq}\epsilon_x l_x \quad (13)$$

where  $S$  is the area of the face, and  $l_x$  is the length of the block. The equivalent homogeneous stiffness,  $K_{eq}$  is analogous to the stiffness of a rod given by  $EA/L$ .

In a porous medium, two longitudinal wave types can exist, each wave type travels in both the structure and the fluid. The ratio of fluid to structural motion in each wave type is known

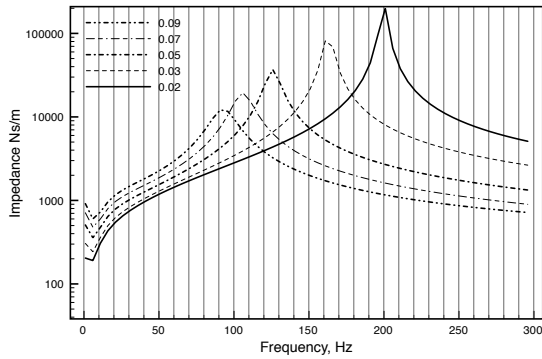


Figure 3. Typical FEA prediction of the input mechanical impedance to the  $35 \times 35 \times 100$ mm melamine block with an 8g mass at 50mm.

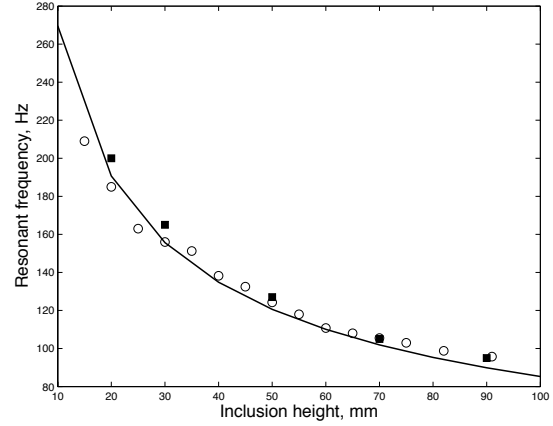


Figure 4. Variation of resonant frequency of an 8 gram mass in a melamine foam block ( $35 \times 35 \times 100$ mm) as a function of the thickness of foam beneath the mass.  $\circ$  data points from experiments. – Equivalent stiffness prediction.  $\blacksquare$  FEA predictions.

and so all the strains in the foam column can be written in terms of the structural strain. The ratio of fluid to structural motion is

$$\mu_{1,2} = \frac{(A + 2N)k_{1,2}^2 - \omega^2 \rho_{11}}{\omega_{12}^2 - Qk_{1,2}^2} \quad (14)$$

Where  $k_{1,2}$  is the wavenumber of the type 1 and 2 waves.  $\rho_{11} = \rho_s - \rho_{12}$ , the difference of structure density and mass coupling,  $\rho_{22} = \phi \rho_f - \rho_{12}$ , the difference of fluid density, weighted by porosity and the mass coupling. The mass coupling term  $\rho_{12}$  is a function of the porosity and the tortuosity. Returning to the derivation of an equivalent stiffness; Rearranging Equation 13 and substituting for stresses using Equation 1-2 it can be expressed as follows

$$K_{eq} = \frac{S}{l_x} \left( 2N + A + Q((1-h)\mu_1 + h\mu_2) + \frac{Q}{(1-h)\mu_1 + h\mu_2} + R \right) \quad (15)$$

The contribution from each wave type is weighted by the porosity under the assumption that the type one wave exists mainly in the structure and the type two wave exists mainly in the fluid. It should be noted that this equivalent stiffness is frequency dependent. The stiffness of a foam block also varies with thickness and so the resonant frequency of the mass inclusions varies with their position in the foam. The resonant frequency of an inclusion was calculated as a function of thickness of material beneath the inclusion and is plotted in Figure 4.

## 5. Comparison of measured and predicted resonant frequencies using experimental, equivalent stiffness and FEA results

### 5.1 Inclusion resonance frequency versus layer thickness

Figure 4 shows the variation in resonant frequency of a mass inclusion vs. layer thickness. The solid line indicates the prediction based on the equivalent stiffness, the solid squares show the

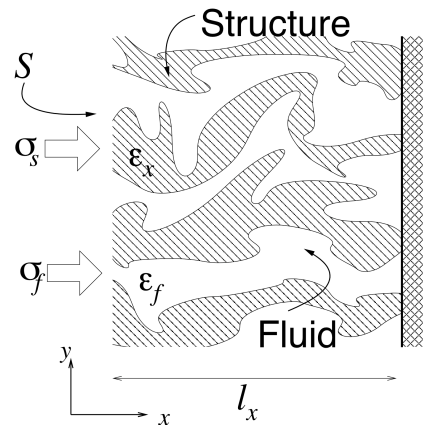


Figure 5. Stresses and strains in a block of foam

FEA result and the circles denote experimental measurements. It can be seen that there is very good agreement between the experimental and equivalent stiffness models. The FEA prediction also matches very well. The result of the simple one dimensional FEA model reinforces the assumptions made in the closed form model. It should also be noted that the low frequency approximations contained in the FEA solution do not effect the accuracy of the result.

## 6. Conclusions

The paper has presented a validation of an FEA and closed form model for the vibration of mass inclusions within poro-elastic layers. It has been shown that the equivalent stiffness model is validated by experimental results. A simple 1D FEA model that includes low frequency approximations of the porous parameters accurately models the phenomena.

*The authors would like to thank the LibMesh open source FEA C++ library. This project was partly supported by NASA grant #NAG-1-02053.*

## References

- [1] M. R. F. Kidner, C. R. Fuller, and B. Gardner, "Increase in transmission loss of single panels by addition of mass inclusions to a poro-elastic layer: Experimental investigation," *Journal of Sound and Vibration*, vol. 294, no. 3, pp. 466–472, 2006.
- [2] M. R. F. Kidner, B. Gardner, and C. Q. Howard, "Improvements in panel insertion loss by addition of random masses embedded in a poro-elastic layer: Modelling procedures," in *ICSV 12*, (Lisbon Portugal), IIAV, 2005.
- [3] J. Allard, *Propagation of sound in porous media*. Elsevier Applied Science, 1993.
- [4] J. S. Bolton and E. R. Green, "Normal incidence sound transmission through double-panel systems lined with relatively stiff partially reticulated polyurethane foam," *Applied Acoustics*, vol. 39, no. 1-2, pp. 23–51, 1993.
- [5] S. Kostek and A. Bayliss, "Finite-difference modeling of acoustic waveforms in a fluid-filled bore-hole surrounded by a biot porous media," *The Journal of the Acoustical Society of America*, vol. 87, no. S1, pp. S113–S113, 1990.
- [6] Y. J. Kang and J. S. Bolton, "Finite element modeling of isotropic elastic porous materials coupled with acoustical finite elements," in *Noise-Con 94*, (Ft Lauderdale FL), pp. 899–904, May 1994.

- [7] N. Atalla, R. Panneton, and P. Debergue, "A mixed displacement-pressure formulation for poroelastic materials," *J. Acoust. Soc. Am.*, vol. 104, no. 3 Pt. 1, pp. 1444–1452, 1998.
- [8] F. C. Sgard, N. Atalla, and R. Panneton, "A modal reduction technique for the finite element formulation of biot's poroelasticity equations in acoustics applied to multilayered structures," *The Journal of the Acoustical Society of America*, vol. 103, no. 5, pp. 2882–2882, 1998.
- [9] N. Atalla, M. A. Hamdi, and R. Panneton, "Enhanced weak integral formulation for the mixed ( $u - p$ ) poroelastic equations," *The Journal of the Acoustical Society of America*, vol. 109, no. 6, pp. 3065–3068, 2001.
- [10] R. Panneton and N. Atalla, "An efficient finite element scheme for solving the three-dimensional poroelasticity problem in acoustics," *The Journal of the Acoustical Society of America*, vol. 101, no. 6, pp. 3287–3298, 1997.
- [11] P. Debergue, R. Panneton, and N. Atalla, "Boundary conditions for the weak formulation of the mixed ( $u, p$ ) poroelasticity problem," *The Journal of the Acoustical Society of America*, vol. 106, no. 5, pp. 2383–2390, 1999.
- [12] Y. J. Kang and J. S. Bolton, "A finite element model for sound transmission through foam-lined double-panel structures," *The Journal of the Acoustical Society of America*, vol. 99, no. 5, pp. 2755–2765, 1996.
- [13] Y. J. Kang, B. K. Gardner, and J. S. Bolton, "An axisymmetric poroelastic finite element formulation," *The Journal of the Acoustical Society of America*, vol. 106, no. 2, pp. 565–574, 1999.
- [14] C. Guigou and C. R. Fuller, "Adaptive feedforward and feedback methods for active passive sound radiation control using smart foam," in *Noise Con 97*, 1997.
- [15] S. J. Estève and M. E. Johnson, "Reduction of sound transmission into a circular cylindrical shell using distribute vibration absorbers and helmholtz resonators," *J. Acoust. Soc. Am.*, vol. 112, pp. 2840–2848, 2002.
- [16] C. R. Fuller and J. D. Jones, "Experiments on reduction of propeller induced interior noise by active control of cylinder vibration," *J. Sound & Vibration*, vol. 112, no. 2, pp. 389–395, 1987.
- [17] R. I. Wright and M. R. F. Kidner, "Vibration absorbers:- a review of applications in interior noise control of propeller aircraft," *J. Vib. Con.*, vol. 10, no. 8, pp. 1221–1231, 2004.
- [18] J. Sun, M. R. Jolly, and M. A. Norris, "Passive, adaptive and active tuned vibration absorbers - a survey," *Transactions of the American Society of Mechanical Engineers*, vol. 117, pp. 234–242, 1995.
- [19] M. Brennan, "Vibration control using a tunable vibration neutraliser," in *Proc Instn Mech Engrs*, vol. 211 part C, pp. 91–108, 1997.
- [20] S. M. Lee, "Normal vibration frequencies of a rectangular two-dimensional array of identical point-masses," *J. Sound. Vib.*, vol. 45(4), pp. 595–600, 1975.
- [21] D. M. Photiadis, "Acoustics of a fluid loaded plate with attached oscillators. part 1. feynman rules," *J. Acoust. Soc. Am.*, vol. 102(1), pp. 348–357, 1997.
- [22] P. Marcotte, C. Fuller, and M. Johnson, "Numerical modeling of distributed active vibration absorbers (dava) for control of noise radiated by a plate," in *Active 2002*, 2002.
- [23] M. Biot, "Theory of propagation if elastic waves in a fluid saturated porous solid. 1. low-frequency range.," *J. Acoust. Soc. Am.*, vol. 28(2), pp. 168–178, 1956.
- [24] D. L. Johnson, J. Koplik, and R. Dashen, "Theory of dynamics permeability and tortuosity in fluid-saturated porous media," *Journal of fluid mechanics*, vol. 176, pp. 379–402, 1987.
- [25] R. Panneton and N. Atalla, "An efficient finite element scheme for solving the three dimensional poro-elasticity problem in acoustics.," *J. Acoust. Soc. Am.*, vol. 101(6), pp. 3287–3297, 1997.
- [26] "Libmesh, a c++ finite element library." <http://libmesh.sourceforge.net>